

INVESTIGATION OF JOHNSON-COOK PARAMETERS OF ALUMINIUM ALLOY 2024-T3

Harant M.^{*}, Jopek M.^{**}, Podaný K.^{***}, Řiháček J.[†]

Abstract: *In this paper the constitutive modeling of mechanical behaviour of aluminium alloy 2024-T3 is presented. This material is often used in automotive, aircraft or aerospace industry. Therefore, to understand the effect of temperature and strain rate on the material properties is crucial. Series of dynamic tests at various strain rates were performed using the Split Hopkinson Pressure Bar. The stress-strain curves have shown moderate strain rate dependence of flow stress. The temperature effect was evaluated using quasi-static compression tests at different temperatures. In this case, the significant thermal softening is observed. Based on these experiments, parameters of the Johnson-Cook material model were determined. A comparative analysis of the numerical simulations and experiments showed a moderate difference between results.*

Keywords: 2024-T3, Johnson-Cook parameters, Hopkinson bar test.

1. Introduction

In the last few decades aluminium alloys have become very popular in automotive, aircraft, and military industry owing to their weight/strength ratio. Aluminium alloy 2024-T3 possesses high ductility, resistance to fatigue crack, or great damage tolerance (Shamchi et al., 2019). Thanks to these properties, it is widely used for wing parts, automobile bodies etc. It is important, especially for these applications, to understand material behaviour at elevated or lower temperature as well as under quasi-static or dynamic loading. All of these factors are involved in the Johnson-Cook material model (Johnson, 1983). To understand the mechanical behaviour and determine the equation parameters, it is necessary to conduct experiments at different temperatures and strain rates. In this paper, Johnson-Cook material model parameters of the 2024-T3 aluminium alloy are investigated based on the experimental procedure. The relevancy of the obtained parameters was subsequently verified by numerical simulation in ANSYS Workbench, module LS-DYNA.

2. Material and methods

The specimens for tests were machined from wire material with diameter of 10 mm. The chemical composition of the alloy provided by the manufacturer is shown in Table 1.

Tab. 1: Chemical composition of aluminium alloy 2024-T3.

Element	Si	Fe	Cu	Mn	Mg	Cr	Zn	Ti	Al
Content	0.06	0.11	4.40	0.48	1.50	0.02	0.05	0.04	Rest

The quasi-static compression tests at room and elevated temperature were conducted on a hydraulic compression-tension testing machine. For the experiments at elevated temperature, a laboratory chamber furnace was used. The specimens are cylinders with diameter of 9 mm and length of 9 mm.

^{*} Ing. Martin Harant: Institute of Manufacturing Technology, Faculty of Mechanical Engineering, Brno University of Technology; Technická 2896/2; 616 69, Brno; CZ, 170977@vutbr.cz

^{**} Ing. Miroslav Jopek, PhD.: Institute of Manufacturing Technology, Faculty of Mechanical Engineering, Brno University of Technology; Technická 2896/2; 616 69, Brno; CZ, jopek@fme.vutbr.cz

^{***} Ing. Kamil Podaný, PhD.: Institute of Manufacturing Technology, Faculty of Mechanical Engineering, Brno University of Technology; Technická 2896/2; 616 69, Brno; CZ, podany@fme.vutbr.cz

[†] Ing. Jan Řiháček, PhD.: Institute of Manufacturing Technology, Faculty of Mechanical Engineering, Brno University of Technology; Technická 2896/2; 616 69, Brno; CZ, rihacek.j@fme.vutbr.cz

The dynamic compression experiments were carried out using the Split Hopkinson Pressure Bar (SHPB), located at the Faculty of Mechanical Engineering, Military University of Technology, Warsaw, Poland. The essential parts of the SHPB device are pneumatic actuator, striker, two bars, damper, and peripheral equipment (strain gauges, oscilloscope, etc.), see Fig. 1. The incident and transmission bar with diameter of 25 mm and length of 2 000 mm are made of the maraging steel. The stress pulses are generated by a striker with diameter of 20 mm and length of 200 mm, made of the same material as the bars. A copper pulse shaper of thickness 1 mm and diameter of 6.14 mm was placed to the impact surface of the incident bar to achieve dynamic equilibrium as quick as possible and to minimize the oscillations during the impact. The specimens are cylinders with a diameter of 9 mm and length of 2, 2.5 and 3 mm, so different strain rates can be achieved for the same experiment settings. Thinner specimens reach faster dynamic equilibrium and inertia effect is suppressed, however friction increases. Nevertheless, the friction effect was not observed during these experiments.

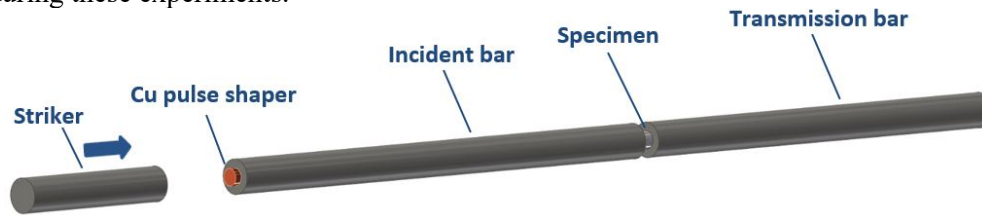


Fig. 1: Schematic of Split Hopkinson Pressure Bar

3. Johnson-Cook material model

The Johnson-Cook material model defines mechanical behaviour of metals in a region of plastic deformation. The flow stress is expressed as the function of strain, strain rate and temperature:

$$\sigma_d = (A + B\varphi^n) \left(1 + C \ln \left(\frac{\dot{\varphi}}{\dot{\varphi}_0} \right) \right) (1 - T^{*m}) \quad (1)$$

where σ_d is the equivalent stress, A is the quasistatic initial yield stress, B is hardening modulus, φ is equivalent plastic strain, n is hardening exponent, C is strain rate coefficient, $\dot{\varphi}$ is strain rate, $\dot{\varphi}_0$ is reference strain rate, m is thermal softening exponent and T^* is homologous temperature defined by $T^* = \frac{T - T_r}{T_m - T_r}$, T is temperature at which experiment is performed, T_r is reference temperature and T_m is melting temperature.

3.1 Determination of parameters A , B and n

The stress-strain curve (Fig. 2) from quasi-static compression test at the reference strain rate of 0.02 s^{-1} and reference temperature of $20 \text{ }^\circ\text{C}$ is used to obtain parameters A , B and n . For this test configuration, the effect of strain rate and temperature is neglected ($T^* = 0$, $\ln \left(\frac{\dot{\varphi}}{\dot{\varphi}_0} \right) = 0$) and Eq. (1) is transformed to Eq. (2).

$$\sigma_d = (A + B\varphi^n) \quad (2)$$

The A parameter represents yield strength for the reference test configuration. The B and n are determined from the Eq.3, which is obtained by rearranging Eq. 2 and taking natural logarithm on both sides:

$$\ln(\sigma_d - A) = n \ln(\varphi) + \ln(B) \quad (3)$$

Plotting $\ln(\sigma_d - A)$ on y-axis and $\ln(\varphi)$ on x-axis, the graph of the linear function in form $y = kx + q$ can be approximated, see Fig. 2. Then the slope $k = n$ and y-intercept $q = \ln(B)$. The parameters are found as $A = 369.86 \text{ MPa}$, $B = 430.57 \text{ MPa}$ and $n = 0.363$.

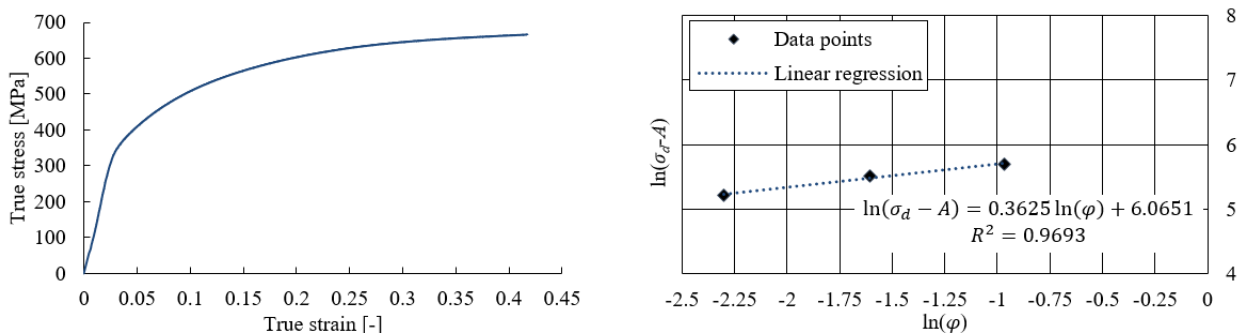


Fig. 2: True stress-strain curve (left), the relationship between $\ln(\sigma_d - A)$ and $\ln(\varphi)$ (right)

3.1 Determination of parameter C

For identification of the C parameter, the set of dynamic tests at reference temperature 20 °C and strain rates of $3\,000\text{ s}^{-1}$, $3\,500\text{ s}^{-1}$ and $4\,000\text{ s}^{-1}$ were conducted. True stress-strain curves for these experiments are presented in Fig. 3. The Eq. 1 can be now simplified ($T^* = 0$) as follows:

$$\sigma_d = (A + B\varphi^n) \left(1 + C \ln \left(\frac{\dot{\varphi}}{\dot{\varphi}_0} \right) \right) \quad (4)$$

A , B and n are known from the previous step and φ value is constant for this case $\varphi = 0.07$. Then the Eq. 4 is modified to:

$$\frac{\sigma_d}{A + B\varphi^n} - 1 = C \ln \left(\frac{\dot{\varphi}}{\dot{\varphi}_0} \right) \quad (5)$$

The parameter C is determined as 0.0232, based on the approximation of the Eq. 5 plot (Fig. 3).

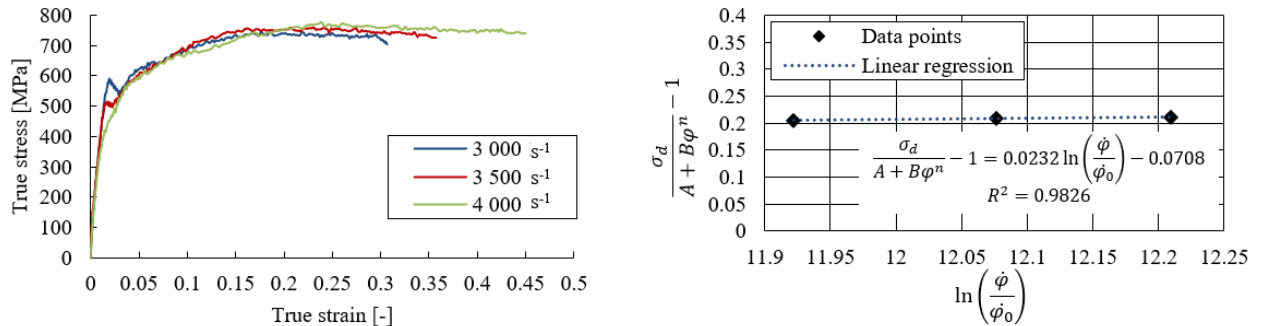


Fig. 3: True stress-strain curves for different strain rates (left), $\left(\frac{\sigma_d}{A + B\varphi^n} - 1 \right) - \ln \left(\frac{\dot{\varphi}}{\dot{\varphi}_0} \right)$ curve (right)

3.1 Determination of parameter m

The parameter m represents temperature effect on flow stress. Therefore, tests at reference strain rate of 0.02 s^{-1} and temperatures of 150 °C and 425 °C were conducted (Fig.4). These experiment configurations ($\ln \frac{\dot{\varphi}}{\dot{\varphi}_0} = 0$) cause following transformation of the Eq. 1:

$$\sigma_d = (A + B\varphi^n)(1 - T^{*m}) \quad (6)$$

The effect of the temperature is analyzed for $\varphi = 0.2$, $T_m = 502\text{ °C}$, and $T_r = 20\text{ °C}$. Then the Eq. 6 can be rearranged as:

$$\ln((A + B\varphi^n) - \sigma_d) = m \ln(T^*) + \ln(A + B\varphi^n) \quad (7)$$

The value of m is obtained from the slope of the approximation function (Fig. 4) as 1.4382.

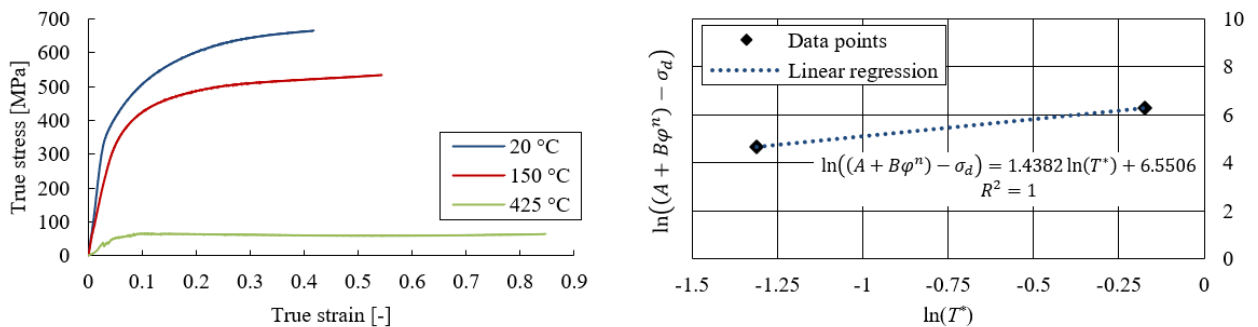


Fig. 4: True stress-strain curves for different temperatures (left), $\ln((A + B\varphi^n) - \sigma_d) - \ln(T^*)$ curve (right)

Since all the parameters had been identified the Johnson-Cook material model can be expressed as:

$$\sigma_d = (369.86 + 430.57\varphi^{0.363}) \left(1 + 0.0233 \ln \frac{\dot{\varphi}}{0.02} \right) (1 - T^{*1.4382}) \quad (8)$$

4. Numerical simulation

For the testing of the relevancy of the Johnson-Cook material model, data from the numerical simulation of the SHPB are compared to experimental results. The numerical simulation was performed in the software ANSYS Workbench, module LS-DYNA, based on the finite element method. 3D geometrical model consists of the striker, bars and, the specimen (according Fig. 1). The specimen mesh is created by elements with an edge length of 0.65 mm. The other components are with the mesh size of 5 mm. The striker, incident and transmission bars were made of the maraging steel defined as an elastic material by Young's modulus $E = 173\,622$ MPa and the Poisson's ratio $\mu = 0.3$. The specimen elastic properties for 2024-T3 were defined by Young's modulus $E = 73\,100$ MPa and the Poisson's ratio $\mu = 0.33$. The Johnson-Cook model defines the specimen hardening behaviour.

The numerical simulation was performed according to the SHPB configurations for various initial specimen length (various strain rates) of 2, 2.5 and 3 mm and the striker velocity for these experiments of $23.7\text{ m}\cdot\text{s}^{-1}$. Frictionless model was used for the contacts. The results of the numerical simulation and real specimen after SHPB (for initial specimen dimensions: $D_0 = 9$ mm and $L_0 = 2.5$ mm) are shown in the Fig. 5.

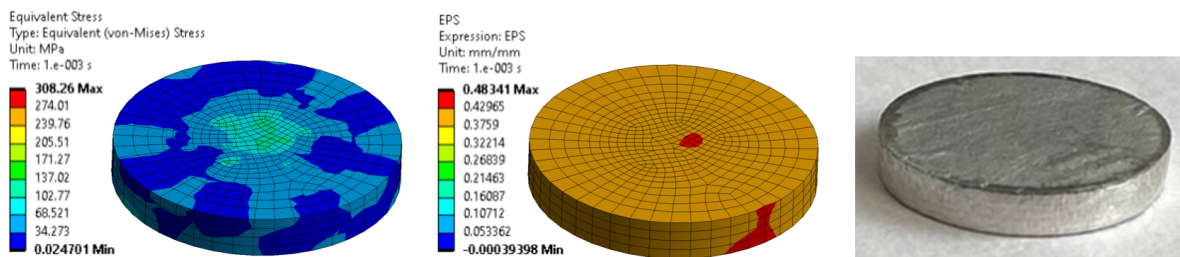


Fig. 5: Equivalent stress (left), equivalent strain (middle), real SHPB specimen (right)

The comparison criteria are the specimen dimensions after the test. These values were measured with a micrometer and the comparison results are summarized in Tab. 2.

Tab. 2: Comparison of the numerical simulation and experimental results

Initial dimensions		$D_0 = 9$ mm, $L_0 = 2$ mm	$D_0 = 9$ mm, $L_0 = 2.5$ mm	$D_0 = 9$ mm, $L_0 = 3$ mm
Final length [mm]	Experiment	1.38	1.83	2.36
	Num. sim.	1.24	1.68	2.13
Percentage change [%]		10.14	8.20	9.75
Final diameter [mm]	Experiment	11.10	10.76	10.41
	Num. sim.	11.58	11.09	10.74
Percentage change [%]		4.14	2.98	3.07

5. Conclusions

In this paper, compression testing of 2024-T3 aluminium alloy is carried out at various temperatures and strain rates to determine five parameters of Johnson-Cook material model. True stress-strain curves obtained from dynamic compression tests conducted on the SHPB show moderate strain rate sensitivity of the alloy. The influence of temperature was investigated only for quasi-static tests. However, this factor has significant effect on the material behaviour in a region of plastic deformation and thermal softening is proved at elevated temperatures. The accuracy of the model was verified using numerical simulation, which is compared with the experimental results. The material behaviour prediction indicates moderate differences between results (maximum percentage change of 10.14 %). To increase the accuracy, the parameters optimization using numerical simulation could be used.

References

- Johnson, G. R. and Cook, W. H. (1983) A Constitutive Model and Data for Metals Subjected to Large Strains, High Strain Rates, and High Temperatures, in: *Proc. 7th Int. Symposium on Ballistics*, Hague, pp. 541-547.
- Shamchi, S. P., Queirós de Melo, F. J. M., Tavares, P. J., and Moreira, P. M. G. P. (2019) Thermomechanical characterization of Alclad AA2024-T3 aluminum alloy using split Hopkinson tension bar. *Mechanics of Materials*, 139, n 103198.